ELSEVIER

www.elsevier.nl/locate/jorganchem

Journal of Organometallic Chemistry 609 (2000) 196–203

Journal of Organometallic Chemistry

The cluster dication $[H_6Ru_4(C_6H_6)_4]^{2+}$ revisited: the first cluster complex containing an intact dihydrogen ligand?

Georg Süss-Fink [a,*1], Laurent Plasseraud [a], Aline Maisse-François [a], Helen Stoeckli-Evans [a], Heinz Berke [b,*2], Thomas Fox [b], Régis Gautier [c,3], Jean-Yves Saillard [c,*4]

[a] *Institut de Chimie, Université de Neuchâtel, Avenue de Bellevaux 51, CH-2000 Neuchâtel, Switzerland*
[b] *Anorganisch-Chemisches Institut der Universität Zürich, Winterthurerstrasse 190, CH-8057 Zurich, Switzerland*
[c] *Laboratoire de Chimie du Solide et Inorganique Moléculaire, UMR-6511, Université de Rennes 1, F-35042 Rennes Cedex, France*

Received 27 January 2000; received in revised form 3 March 2000

Dedicated to Professor Heinrich Vahrenkamp on the occasion of his 60th birthday

Abstract

A low-temperature ^{1}H-NMR study suggests the tetranuclear cluster dication $[H_6Ru_4(C_6H_6)_4]^{2+}$ (**1**) to contain an H_2 ligand that undergoes, upon warming of the solution, an intramolecular exchange with the four hydride ligands at the Ru_4 framework. Whereas two of the three NMR signals at -120°C in the hydride region show T_1 values in the range 200–300 ms, the least deshielded resonance at $\delta = -17.33$ ppm exhibits a T_1 value of only 34 ms, characteristic of an H_2 ligand. A re-examination of the single-crystal X-ray structure analysis of the chloride salt of **1** supports this interpretation by a short distance of 1.14(0.15) Å between two hydrogen atoms coordinated as a H–H ligand in a side-on fashion to one of the triangular faces of the Ru_4 tetrahedron. The distance between one of the two hydrogen atoms of the H_2 ligand and one of the four hydride ligands is also very short [1.33(0.15) Å], suggesting an additional $H_2\cdots H$ interaction. The presence of this H_3 unit over one of the three Ru_3 faces in **1** may explain the deformation of the Ru_4 skeleton from the expected tetrahedral symmetry. Density functional theory (DFT) calculations on **1** indicate a very soft potential energy surface associated with the respective displacement of the three interacting cofacial hydrogen atoms. In accordance with these results, the cluster dication **1** tends to loose molecular hydrogen to form the cluster dication $[H_4Ru_4(C_6H_6)_4]^{2+}$ (**2**). The equilibrium between **1** and **2** can be used for catalytic hydrogenation reactions.

Keywords: Dihydrogen ligand; Cluster; Ruthenium; NMR T_1 measurements; Molecular structure; Density functional calculations

1. Introduction

One of the most fascinating aspects of transition metal chemistry involves the coordination of hydride ligands. The first hydride complexes, $HCo(CO)_4$ and $H_2Fe(CO)_4$, were reported by Hieber et al. in the 1930s [1], but their structures and the nature of the metal–hydrogen bond were unclear until much later. Today thousands of transition metal hydride complexes are known [2], they are of outstanding importance for many catalytic reactions [3]. In transition metal cluster chemistry, hydride ligands are encountered not only as μ_1-terminal ligands but more often as μ_2-bridging or μ_3-capping ligands, sometimes even as μ_n-interstitial ligands encapsulated in the metal framework [4].

The spectacular discovery of the first dihydrogen complex, $(H_2)W(CO)_3(P^iPr_3)_2$ by Kubas et al. in 1984 [5] has had a strong impact on coordination and hydrogenation chemistry [6]. It is now generally accepted that molecular hydrogen can be coordinated to a metal centre as an intact unit, which may then undergo H–H bond cleavage to form hydrido ligands [7]. Theoretical

[1] *Corresponding author. Tel.: +41-32-7182400; fax: +41-32-7182511; e-mail: georg.suess-fink@ich.unine.ch
[2] *Corresponding author.
[3] Present address: Département de Physicochimie, Ecole Nationale Supérieure de Chimie de Rennes, F-35700 Rennes Cedex, France.
[4] *Corresponding author.

0022-328X/00/$ - see front matter
PII: S0022-328X(00)00171-6

studies show that in dihydrogen complexes the coordination of the H_2 ligand can be described in terms of a $H_2 \rightarrow M$ σ interaction combined with a $M \rightarrow H_2$ π back-donation [8]. Mono- and dimetallic polyhydrogen complexes have also been theoretically investigated by Burdett and co-workers who suggested the possibility of existence of open and closed coordinated H_3 triangles [9].

The unambiguous characterisation of dihydrogen complexes is not trivial because it is very often difficult to distinguish an intact H_2 ligand from two hydride ligands. Neutron diffraction is the most adequate method to characterise H_2 complexes [10], its application being limited, however, by the restricted availability of neutron diffraction facilities, the large crystal sizes necessary and the long measuring times. In some cases, X-ray crystallography gives useful data, in particular if the crystal structure analysis is carried out at low-temperature [11]. Among other methods (IR, NMR), relaxation time measurements of the proton NMR signals are the most meaningful criteria for distinguishing a H_2 from two H ligands: The ^1H resonances of H_2 ligands have much shorter T_1 values than those of hydride ligands, the rapid relaxation time being due to the short H–H distance in the H_2 ligand [12]. By applying the T_1 criterion, several di- or oligohydride complexes known before have been reinterpreted in terms of H_2 complexes [13].

The cluster dication $[H_6Ru_4(C_6H_6)_4]^{2+}$ (**1**) has a rather complex history: we obtained **1** in 1993 from the reaction of a (benzene)ruthenium dichloride dimer with molecular hydrogen in aqueous solution under high pressure conditions. In the single-crystal X-ray structure analysis of the chloride salt of **1** (violet crystals), we found only four of the six hydrides, which prompted us to publish **1** erroneously as $[H_4Ru_4(C_6H_6)_4]^{2+}$ [14]. As we obtained this tetrahydrido cluster dication $[H_4Ru_4(C_6H_6)_4]^{2+}$ (**2**) in 1994, the chloride salt (black–brown crystals) being distinctly different of that of **1**, we established the formula of $[H_6Ru_4(C_6H_6)_4]^{2+}$ for **1** on the basis of the integral ratio of the proton NMR signal of the hydrides with respect to that of the benzene protons (6:24). Finally, we were able to locate the six hydrides in the crystal structure analysis of the *para*-cymene analogue $[H_6Ru_4(p\text{-Me–}C_6H_4\text{–}Pr^i)_4]^{2+}$ (**3**) (perchlorate salt) [15].

The deformation of this tetranuclear cluster from tetrahedral symmetry in the crystal remained mysterious: the Ru_4 tetrahedron is distinctly distorted, and the six hydride ligands were not found as μ_2-bridges over the six Ru–Ru bonds, as expected from the single hydride resonance of $\delta = -15.03$(s) and $\delta = -15.83$(s) ppm observed for **1** and **3**, respectively, in D_2O solution [15]. This contradiction induced us to again study the hexahydrido cluster $[H_6Ru_4(C_6H_6)_4]^{2+}$ (**1**) by low-temperature ^1H-NMR spectroscopy, low-temperature T_1 measurements, X-ray crystallography and by density functional theory (DFT) calculations.

2. Results and discussion

2.1. Synthesis

The cluster dication $[H_6Ru_4(C_6H_6)_4]^{2+}$ (**1**) is accessible by high-pressure reaction of an aqueous solution of $(C_6H_6)_2Ru_2Cl_4$ with H_2 (60 bar, 55°C). It was found according to Eq. (1) along with small quantities of the tetrahydrido cluster $[H_4Ru_4(C_6H_6)_4]^{2+}$ (**2**) and can be isolated from the aqueous solution as the hexafluorophosphate salt in an analytically pure form. The chloride salt (violet crystals) gives better crystals, suitable for a single-crystal X-ray structure analysis, but it is never pure since the chloride salt of **2** (black–brown crystals) crystallises simultaneously from water. The tetrahydrido cluster $[H_4Ru_4(C_6H_6)_4]^{2+}$ (**2**) is obtained exclusively under low-pressure conditions (1.5 bar, 20°C) according to Eq. (2).

$$2\ Ru_2(C_6H_6)_2Cl_4 + 6\ H_2 \longrightarrow \underset{(1)}{[H_6Ru_4(C_6H_6)_4]^{2+}} + 8\ Cl^- + 6\ H^+ \quad (1)$$

$$2\ Ru_2(C_6H_6)_2Cl_4 + 5\ H_2 \longrightarrow \underset{(2)}{[H_4Ru_4(C_6H_6)_4]^{2+}} + 8\ Cl^- + 6\ H^+ \quad (2)$$

With an electron count of 60e, the hexahydrido cluster **1** is an electron-precise species in accordance with the noble gas rule. By contrast, the tetrahydrido cluster **2** contains only 58e and represents an electron-deficient system. Nevertheless, the electron-precise cluster cation **1** is easily oxydized by air (1 bar, 20°C) to form the electron-deficient cluster dication **2** and water (Eq. (3)). The dication **2** can be reduced, in turn, with molecular hydrogen to give the dication **1** under forcing conditions (60 bar, 55°C) according to Eq. (4). Both reactions take place in aqueous solution. The equilibrium between **1** and **2** can be used for the catalytic hydrogenation of benzene and benzene derivatives to the corresponding cyclohexanes under biphasic conditions [16].

$$\underset{(1)}{[H_6Ru_4(C_6H_6)_4]^{2+}} + 1/2\ O_2 \longrightarrow \underset{(2)}{[H_4Ru_4(C_6H_6)_4]^{2+}} + H_2O \quad (3)$$

$$\underset{(2)}{[H_4Ru_4(C_6H_6)_4]^{2+}} + H_2 \longrightarrow \underset{(1)}{[H_6Ru_4(C_6H_6)_4]^{2+}} \quad (4)$$

Crystals of $[H_6Ru_4(C_6H_6)_4]Cl_2$ (cation **1**) suitable for a single-crystal X-ray structure analysis were grown in water under hydrogen pressure (3 bar).

2.2. NMR spectroscopy

In order to investigate the nature of the six metal-bonded hydrogen atoms in the cluster dication **1**, we prepared the chloride salt $[H_6Ru_4(C_6H_6)_4]Cl_2$ and studied the ^{1}H-NMR spectra of **1** (in a 1:1 mixture of tetrahydrofurane-d_8 and methanol-d_4) over a temperature range $+25$°C to -120°C.

At room temperature (r.t.), the ^{1}H-NMR spectrum of **1** exhibits one hydride resonance at $\delta = -14.9$ ppm due to fast exchange on the NMR time scale. At -120°C, by contrast, three distinct hydride signals can be resolved (Fig. 1). At this low temperature, one-dimensional ^{1}H exchange experiments have been performed using a standard ^{1}H-NOE sequence. Saturation via selective irradiation onto the low field signal at $\delta = -12.9$ ppm leads to saturation transfer onto the signal at $\delta = -17.0$ ppm, the signals at $\delta = -15.0$ and $\delta = -17.4$ ppm are not affected (Fig. 2). In addition, saturation of the signal at $\delta = -15.0$ ppm does not affect any other signal. Therefore, and due to intensity considerations, there are three different hydrogen sites in the cluster, which are occupied in a 2:2:2 ratio ($\delta = -12.9$, -17.0 and -17.4 ppm), whereas the tiny signal at $\delta = -15.0$ ppm is due to a small amount of impurity.

The determination of the longitudinal T_1 relaxation times yields normal relaxation behaviour for the resonances at $\delta = -12.9$ and $\delta = -17.0$ ppm with T_1 values of 310 and 190 ms, whereas the T_1 time for the resonance at -17.4 ppm amounts to only 34 ms, thus being in the typical range of non-classical dihydrogen complexes. As shown in the exchange experiments, there is no exchange between the dihydrogen rotor and the classical hydrides at low temperature, whereas there is a fast exchange between all hydrogen sites at r.t., as demonstrated by deuteration experiments. For this purpose a sample of the chloride salt of **1** was sealed in a

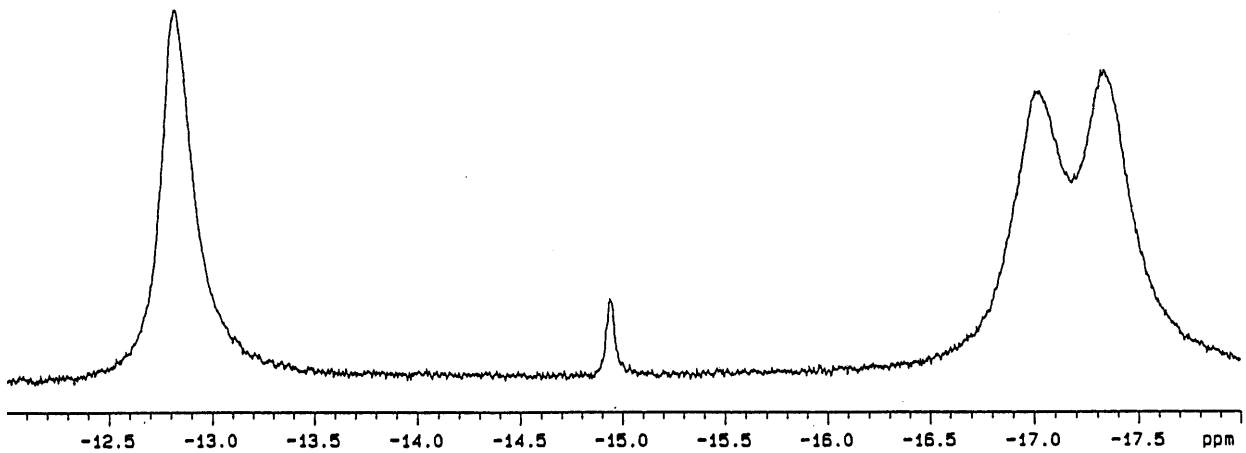

Fig. 1. ^{1}H-NMR spectrum of $[H_6Ru_4(C_6H_6)4]^{2+}$ (**1**) at -120°C (region from -12.5 to -17.5 ppm), the signal at $\delta = -15.0$ ppm being due to an impurity.

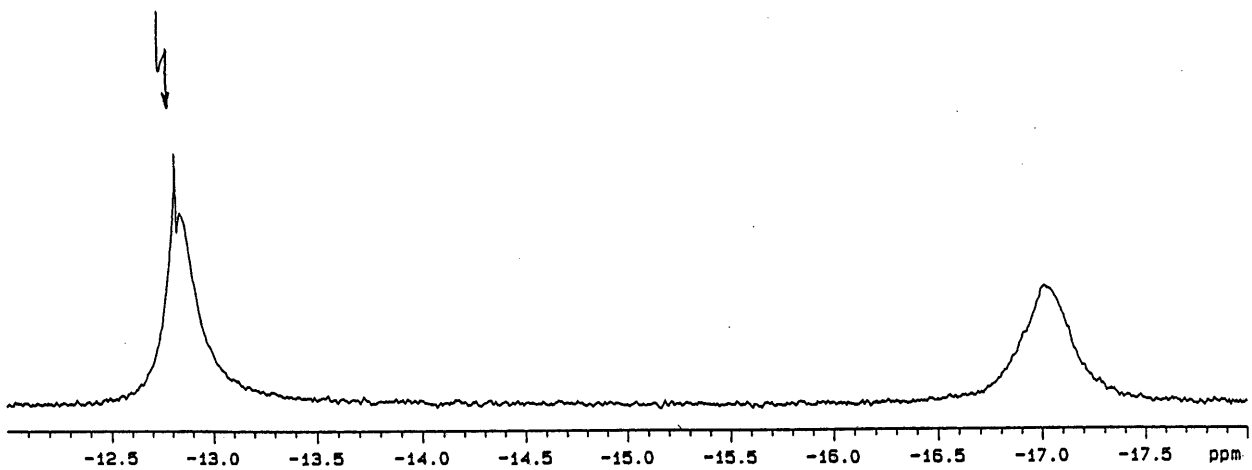

Fig. 2. Selective irradiation at $\delta = -12.9$ ppm leads to saturation at $\delta = -17.0$ ppm.

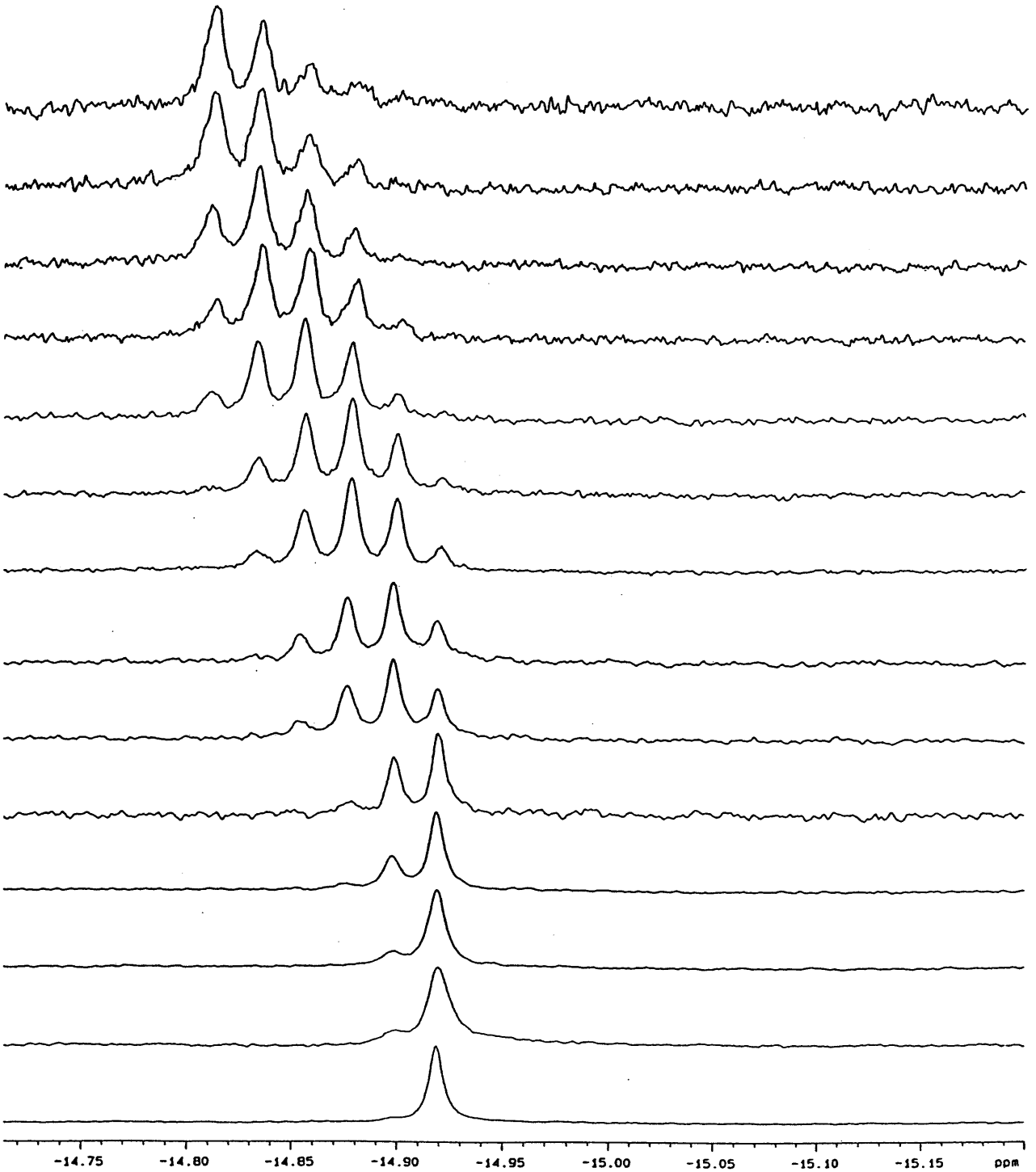

Fig. 3. ^{1}H-NMR of $[H_6Ru_4(C_6H_6)_4]^{2+}$ (**1**) at room temperature; the degree of deuteration gradually increasing between 15 min (bottom) and 6 h (top) under D_2 atmosphere.

D_2 atmosphere. Immediately after preparation of the sample, the ^{1}H-NMR spectrum shows, at r.t., only one hydride signal at $\delta = -14.9$ ppm (Fig. 3), which slowly decreases within several hours, while new signals appear at lower field in a range between 6.3 and 6.9 Hz. The latter ones are due to the gradual formation of H/D-isotopomers of **1**, the degree of deuteration increasing with lower field. The observation of all six ^{1}H-NMR detectable H/D-isotopomers (H_6D_0 to H_1D_5) in **1** is indicative of an exchange between classical and non-classical hydrides at r.t., because the number of deuterium per complex increases step by step.

We also tried to resolve the ^1J(H, D) coupling of the non-classical dihydrogen rotor of partially deuterated **1**

in order to estimate the H–H distance. Unfortunately, this attempt failed, presumably because the extremely low temperature of −120°C, necessary for freezing out the fluxional processes, causes line shapes much too broad to show the ^1J(H, D) coupling.

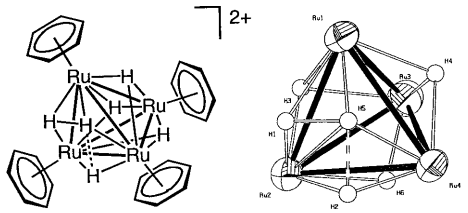

Fig. 4. Ru_4H_6 core of $[H_6Ru_4(C_6H_6)_4]^{2+}$ (**1**) (SCHAKAL plot).

Table 1
Selected bond lengths (Å) and angles (°) for $[H_6Ru_4(C_6H_6)_4]Cl_2$

Ru(1)–C(4)	2.178(9)	C(11)–C(12)	1.428(18)
Ru(1)–C(3)	2.184(9)	C(13)–C(18)	1.309(17)
Ru(1)–C(5)	2.187(9)	C(13)–C(14)	1.382(17)
Ru(1)–C(1)	2.190(8)	C(14)–C(15)	1.367(18)
Ru(1)–C(6)	2.192(8)	C(15)–C(16)	1.42(2)
Ru(1)–C(2)	2.200(8)	C(16)–C(17)	1.42(2)
Ru(1)–Ru(3)	2.7533(9)	C(17)–C(18)	1.341(19)
Ru(1)–Ru(2)	2.7918(9)	C(19)–C(20)	1.377(13)
Ru(1)–Ru(4)	2.8139(9)	C(19)–C(24)	1.384(14)
Ru(2)–C(8)	2.170(9)	C(20)–C(21)	1.394(13)
Ru(2)–C(11)	2.176(9)	C(21)–C(22)	1.370(14)
Ru(2)–C(10)	2.181(9)	C(22)–C(23)	1.401(15)
Ru(2)–C(9)	2.185(9)	C(23)–C(24)	1.391(14)
Ru(2)–C(7)	2.196(8)		
Ru(2)–C(12)	2.199(8)		
Ru(2)–Ru(4)	2.8000(8)		
Ru(2)–Ru(3)	2.8154(9)		
Ru(3)–C(15)	2.170(10)	Ru(3)–Ru(1)–Ru(2)	61.02(2)
Ru(3)–C(16)	2.170(11)	Ru(3)–Ru(1)–Ru(4)	59.15(2)
Ru(3)–C(14)	2.171(10)	Ru(2)–Ru(1)–Ru(4)	59.93(2)
Ru(3)–C(17)	2.177(10)	Ru(1)–Ru(2)–Ru(4)	60.43(2)
Ru(3)–C(13)	2.190(10)	Ru(1)–Ru(2)–Ru(3)	58.82(2)
Ru(3)–C(18)	2.193(10)	Ru(4)–Ru(2)–Ru(3)	58.60(2)
Ru(3)–Ru(4)	2.7481(9)	Ru(4)–Ru(3)–Ru(1)	61.53(2)
Ru(4)–C(23)	2.184(8)	Ru(4)–Ru(3)–Ru(2)	60.42(2)
Ru(4)–C(24)	2.185(8)	Ru(1)–Ru(3)–Ru(2)	60.16(2)
Ru(4)–C(19)	2.193(7)	Ru(3)–Ru(4)–Ru(2)	60.98(2)
Ru(4)–C(20)	2.194(7)	Ru(3)–Ru(4)–Ru(1)	59.33(2)
Ru(4)–C(21)	2.198(9)	Ru(2)–Ru(4)–Ru(1)	59.64(2)
Ru(4)–C(22)	2.201(9)		
C(1)–C(6)	1.367(15)		
C(1)–C(2)	1.394(15)		
C(2)–C(3)	1.390(15)		
C(3)–C(4)	1.421(16)		
C(4)–C(5)	1.366(16)		
C(5)–C(6)	1.377(15)		
C(7)–C(12)	1.337(16)		
C(7)–C(8)	1.370(14)		
C(8)–C(9)	1.326(15)		
C(9)–C(10)	1.364(17)		
C(10)–C(11)	1.425(19)		

Table 2
Ruthenium···hydride distances (average estimated S.D. ± 0.10 Å) and hydride···hydride distances (average estimated S.D. ± 0.15 Å) for $[H_6Ru_6(C_6H_6)_4]Cl_2$

Distances Ru···H		Distances H···H	
Ru1–H1	1.87	H1–H2	1.67
Ru1–H3	1.80	H1–H3	1.95
Ru1–H4	1.91	H1–H4	3.01
Ru1–H5	1.68	H1–H5	1.14
Ru2–H1	1.69	H1–H6	2.71
Ru2–H2	1.80	H2–H3	2.76
Ru2–H3	1.61	H2–H4	2.88
Ru2–H6	1.80	H2–H5	1.33
Ru3–H3	2.06	H2–H6	1.88
Ru3–H4	1.75	H3–H4	2.50
Ru3–H6	1.80	H3–H5	2.34
Ru4–H2	1.61	H3–H6	2.25
Ru4–H4	1.84	H4–H5	2.25
Ru4–H5	1.79	H4–H6	2.18
Ru4–H6	1.66	H5–H6	2.36

2.3. X-ray analysis

In order to confirm the presence of a dihydrogen ligand in the cluster dication $[H_6Ru_4(C_6H_6)_4]^{2+}$ (**1**), we undertook a single-crystal X-ray analysis of $[H_6Ru_4(C_6H_6)_4]Cl_2$, which enabled us to locate all six metal-bonded hydrogen atoms. Further attempts to obtain suitable crystals for a low-temperature analysis were not successful. We also attempted a neutron diffraction study which failed, since the single-crystal of $[H_6Ru_4(C_6H_6)_4]Cl_2$ was not stable or big enough to support the neutron bombardment over a period of 13 days even at 4 K. We therefore depend on the less precise r.t. X-ray data for the hydrogen–hydrogen distances.

The molecular structure of **1** is depicted in Fig. 4, important bond lengths and angles are given in Table 1. The Ru_4 framework in **1** shows a distorted tetrahedral arrangement with Ru–Ru bond lengths varying between 2.7481(9) and 2.8154(9) Å. The aromatic rings coordinate in the usual η^6 fashion to the respective Ru atoms and are planar within the experimental error. All six metal-bonded hydrogen atoms could be located and refined. Their interatomic distances are given in Table 2.

Neutron diffraction studies of dihydrogen complexes have revealed hydrogen–hydrogen distances of typically 0.8–1.1 Å, in some cases ('stretched' H_2 ligands) distances up to 1.3 Å or even longer [10]. The analysis of the hydrogen–hydrogen distances of **1** shows a very close contact between H1 and H5, 1.14(0.15) Å, which we interpret in terms of a H_2 ligand coordinated in a μ_3-η^2 fashion ('side-on') to the triangular face Ru1–Ru2–Ru4 of the Ru_4 tetrahedron. A second short distance of 1.33(0.15) Å between H2 and H5 can be

considered as an additional $H_2\cdots H$ interaction with the μ_2 hydrido bridge H5 over the Ru1–Ru4 bond (Fig. 4). Thus an H_3 unit sitting over the Ru1–Ru2–Ru4 face seems to be already preformed in the solid state as a starting point of the fluxionality of all six metal-bonded hydrogen atoms observed in solution.

2.4. Theoretical investigations

In order to evaluate theoretically the H···H distances in complex **1**, DFT calculations have been performed. A full geometry optimisation of **1** under the C_s symmetry constraint led to the geometry shown in Fig. 5. A good agreement was obtained with the experimental Ru–Ru, C–C, C–H, and Ru–(μ^3-H) bond distances. The calculated Ru–C distances (2.24–2.29 Å) were found to be slightly longer (0.05 Å) than the experimental ones from the X-ray data. The computed contacts between the three co-facial hydrogen atoms (2×1.95 and 1.87 Å) are longer than those resulting from the X-ray analysis. The shortest can be considered as indicative of a very weak H–H interaction.

With a weak bonding interaction, the H–H separation is expected to be very sensitive to small geometrical variations of the cluster cage. Since the optimised cluster cage is slightly different from the experimental one, we have also carried out the optimisation of the three co-facial hydrogen locations assuming the rest of the cluster being frozen in its experimental geometry, which is of C_1 symmetry. Two of the resulting three H···H distances are significantly shorter (1.66, 1.76, and 2.12 Å), suggesting weak but significant bonding interactions. The energy gain with respect to the full experimental structure is 9 kcal mol^{-1}.

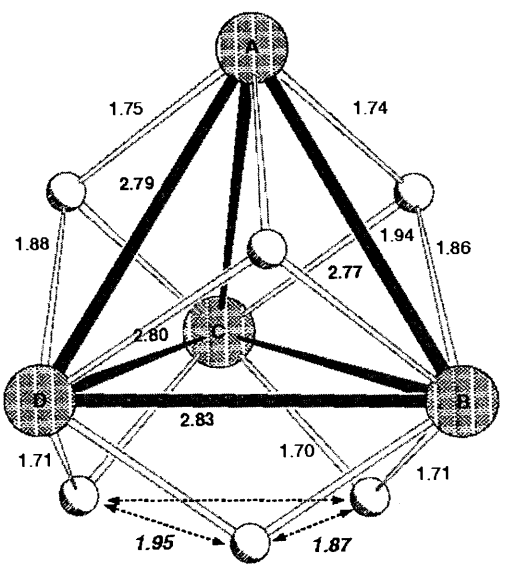

Fig. 5. The DFT optimised structure of complex **1** assuming C_s symmetry. The large spheres are Ru atoms and the small spheres are H atoms. The symmetry plane contains Ru(A), Ru(B), and the middle of the Ru(C)–Ru(D) vector.

A partial exploration of the potential energy surface associated with the displacement of the co-facial H atoms indicates that this surface is rather flat around its minimum, i.e. significant variations of the H···H separations have little effect on the total energy of **1**. Taking all the experimental and theoretical data together, one can conclude that the X-ray measurements lead probably to underestimated H–H distances, whereas DFT calculations tend to overestimate them slightly. In any case, there must be significant interactions between the three co-facial hydrogen atoms.

3. Experimental

The complex $[Ru_2(\eta^6\text{-}C_6H_6)Cl_2]_2$ was synthesized according to a published method [17]. Water was bidistilled prior to use. The ^{1}H-NMR spectra were recorded using a Varian Gemini 200 BB instrument and referenced to TMS.

3.1. Syntheses

3.1.1. $[H_6Ru_4(\eta^6\text{-}C_6H_6)_4]Cl_2$ (cation **1**)

A suspension of $[Ru(\eta^6\text{-}C_6H_6)Cl_2]_2$ (150 mg, 0.30 mmol) in H_2O (20 cm^3) was hydrogenated in a stainless-steel autoclave at 55°C under a pressure of 60 atm. After 14 h the autoclave was cooled, the pressure was released, and the violet solution was filtered. The solution was concentrated under reduced pressure (10^{-3} mbar, 40°C) in alternation with pressurising with H_2 (3 bar). Crystallisation at 2°C in a pressure Schlenk tube under an atmosphere of H_2 (3 bar) gave the chloride salt of **1** as dark violet crystals (81 mg, 65%). The chloride salt of **1** was contaminated by a small amount of $[H_4Ru_4(\eta^6\text{-}C_6H_6)_4]Cl_2$ (cation **2**), as evidenced by the NMR spectrum. Nevertheless, **1** can be isolated in an analytically pure form as the hexafluorophosphate salt $[H_6Ru_4(\eta^6\text{-}C_6H_6)_4][PF_6]_2$ by treatment of an aqueous solution of $[H_6Ru_4(\eta^6\text{-}C_6H_6)_4]Cl_2$ with an excess of NH_4PF_6, followed by filtration of the precipitate. ^{1}H-NMR (acetone-d_6) δ (ppm): 6.23 (s, 24H), −14.73 (s, 6H).

3.1.2. $[H_4Ru_4(\eta^6\text{-}C_6H_6)_4]Cl_2$ (cation **2**)

The filtered violet reaction mixture obtained after the hydrogenation step in the synthesis of **1** was evaporated to dryness, dissolved in methanol (10 cm^3) and stirred under air for 1 day. Evaporation of most of the solvent under reduced pressure, followed by crystallisation at 2°C, gave the chloride salt of **2** as black–brown crystals (65 mg, 55%). ^{1}H-NMR (D_2O) δ (ppm): 6.02 (s, 24H), −17.38 (s, 4H). The tetrafluoroborate salt of **2** can be obtained directly by placing $[Ru(\eta^6\text{-}C_6H_6)Cl_2]_2$ and $NaBF_4$ in water in a pressure Schlenk tube and stirring the mixture under an H_2 pressure of 1.5 atm at r.t. for

Table 3
Crystal data table for $[H_6Ru_4(\eta^6\text{-}C_6H_6)_4]Cl_2$

Compound	$[H_6Ru_4(\eta^6\text{-}C_6H_6)_4]Cl_2\cdot 5H_2O$
Empirical formula	$C_{24}H_{40}Cl_2O_5Ru_4$
Crystal shape	Block
Crystal colour	Purple
Crystal size (mm)	$0.76\times0.76\times0.65$
Crystal system	Monoclinic
M	883.82
Space group	$P2_1/n$
Unit cell dimensions	
a (Å)	9.463(2)
b (Å)	17.675(3)
c (Å)	17.501(2)
α (°)	90
β (°)	96.870(10)
γ (°)	90
V (Å^3)	2906.2(9)
Z	4
D_{calc} (g cm^{-3})	2.021
μ(Mo–K$_\alpha$) (mm^{-1})	2.254
F(000)	1712
θ scan range (°)	1.64–25.02
T (K)	293(2)
N standards	2
Intensity variation (%)	1
Reflections measured	5122
Independent reflections	5122
Reflections observed $[I>2\sigma(I)]$	4571
Final R indices $[I>2\sigma(I)]$	$R_1=0.0429,\ wR_2=0.1161$
R indices (all data)	$R_1=0.0496,\ wR_2=0.1213$
Goodness-of-fit	1.111
Maximum Δ/σ	0.004
Residual density: maximum, minimum $\Delta\rho$ (e Å^{-3})	1.113, −1.242

a period of 120 h. Filtration, extraction with acetonitrile, and evaporation of the solvent under reduced pressure yielded the pure product $[H_4Ru_4(\eta^6\text{-}C_6H_6)_4][BF_4]_2$. ^{1}H-NMR (acetonitrile-d_3) δ (ppm): 5.83 (s, 24H), −17.66 (s, 4H).

3.2. NMR experiments

The NMR experiments were enregistrated on a 300 MHz, Varian Gemini-300 and on a Varian Gemini 2000. $[H_6Ru_4(\eta^6\text{-}C_6H_6)_4]Cl_2$ (15 mg) was dissolved in a 1:1 mixture of THF-d_8 and MeOH-d_4; the sealed samples were stored at −80°C.

3.3. Crystallography

Suitable crystals of $[H_6Ru_4(\eta^6\text{-}C_6H_6)_4]Cl_2$ were grown from water as purple blocks. Intensity data were collected at r.t. on a Stoe AED2 4-circle diffractometer using Mo–K$_\alpha$ graphite monochromated radiation (λ = 0.71073 Å) with $\omega/2\Theta$ scans in the 2Θ range 4–51°. The structure was solved by direct methods using the programme SHELXS-97 [18]. The refinement and all further calculations were carried out using SHELXL-97 [19]. The hydride H-atoms were located from difference Fourier maps and initially refined isotropically. They were held fixed in the final cycles of least-squares refinement. The aromatic H-atoms were included in calculated positions and treated as riding atoms using SHELXL-97 default parameters. The water H-atoms could not be located. The non-H atoms were refined anisotropically, using weighted full-matrix least-squares on F^2.

Table 2 gives a list of Ru···H and H···H distances.

Crystallographic and selected experimental data for cation **1** are given in Table 3.

The molecular structure and crystallographic numbering scheme are illustrated in the PLATON [20] drawings.

3.4. Theoretical calculations

Density functional theory calculations were carried out using the Amsterdam density functional (ADF) program [21] developed by Baerends and co-workers [22]. Becke exchange [23] and Perdew correlation [24] non-local gradient corrections were included in the local density approximation [25]. The geometry optimisation was based on the method developed by Versluis and Ziegler [26]. The Slater-type basis was of double-ς quality for C and H atoms of the phenyl ligands and of triple-ς quality for Ru and other H atoms. The Ru (1s–4p) and C (1s) cores were kept frozen [27]. A single-ς 5p polarisation function was included in the Ru valence set, as well as a single-ς 3d one in the C valence set, and a single-ς 2p one in the H basis set.

4. Supplementary material

Crystallographic data for the structural analysis have been deposited with the Cambridge Crystallographic Data Centre, CCDC no. 139231 for compound **1**. Copies of this information may be obtained free of charge from The Director, CCDC, 12 Union Road, Cambridge CB2 1EZ (Fax: +44-1223-336033; e-mail: deposit@ccdc.cam.ac.uk or http://www.ccdc.cam.ac.uk).

Acknowledgements

The authors are grateful to Professor Karl Wieghardt and to Dr E. Bill, Max-Planck-Institut für Strahlenchemie, Mülheim (Ruhr), for magnetic susceptibility measurements. Financial support from the Swiss National Science Foundation and a generous loan of ruthenium chloride hydrate from the Johnson Matthey Technology Centre are gratefully acknowledged.

References

[1] (a) W. Hieber, Naturwissenschaften 19 (1931) 360. (b) W. Hieber, F. Leutert, Ber. Dtsch. Chem. Ges. 64 (1931) 2832. (c) W. Hieber, F. Leutert, Z. Anorg. Allg. Chem. 204 (1932) 145. (c) W. Hieber, Z. Elektrochem. 40 (1934) 158. (d) W. Hieber, H. Schulten, K. Krämer, Angew. Chem. 49 (1936) 463. (e) W. Hieber, H. Schulten, K. Krämer, Z. Anorg. Allg. Chem. 232 (1937) 17.

[2] (a) G.G. Hlatky, R.H. Crabtree, Coord. Chem. Rev. 65 (1985) 1. (b) K. Yvon, Chimia 52 (1998) 613.

[3] (a) B.R. James, Homogeneous Hydrogenation, Wiley, New York, 1973. (b) W.L. Gladfelter, K.J. Roesselet, in: D.F. Shriver, H.D. Kaesz, R.D. Adams (Eds.), The Chemistry of Metal Cluster Complexes, VCH, New York, 1990 (Chapter 7).

[4] (a) S. Aime, M. Botta, R. Gobetto, L. Milone, D. Osella, R. Gellert, E. Rosenberg, Organometallics 14 (1995) 3693. (b) A.P. Humphries, H.D. Kaesz, Prog. Inorg. Chem. 25 (1979) 145.

[5] G.J. Kubas, R.R. Ryan, B.I. Swanson, P.J. Vergamini, H.J. Wasserman, J. Am. Chem. Soc. 106 (1984) 451.

[6] (a) G.J. Kubas, Acc. Chem. Res. 21 (1988) 120. (b) H. Crabtree, Acc. Chem. Res. 23 (1990) 95. (b) G. Jessop, R.H. Morris, Coord. Chem. Rev. 121 (1992) 155. (c) M. Heinekey, W.J. Oldham Jr., Chem. Rev. 93 (1993) 913. (d) H. Crabtree, Angew. Chem. Int. Ed. Engl. 32 (1993) 789. (e) R. Bau, R.G. Teller, S.W. Kirtley, T.F. Koetzle, Acc. Chem. Res. 12 (1979) 180. (f) D.G. Gusev, H. Berke, Chem. Ber. 129 (1996) 1143. (g) D.G. Gusev, R. Hübener, P. Burger, O. Orama, H. Berke, J. Am. Chem. Soc. 119 (1997) 3716.

[7] (a) R.H. Crabtree, M. Lavin, L. Bonneviot, J. Am. Chem. Soc. 108 (1986) 4032. (b) J.M. Millar, R.V. Kastrup, M.T. Melchior, I.T. Horvath, C.D. Hoff, R.H. Crabtree, J. Am. Chem. Soc. 112 (1990) 9643.

[8] (a) P.J. Hay, Chem. Phys. Lett. 103 (1984) 466. (b) P.J. Hay, J. Am. Chem. Soc. 109 (1987) 705. (c) J.-Y. Saillard, R. Hoffmann, J. Am. Chem. Soc. 106 (1984) 2006. (d) Y. Jean, O. Eisenstein, F. Volatron, B. Maouche, F. Sefta, J. Am. Chem. Soc. 108 (1986) 6587. (e) F. Maseras, M. Duran, A. Lledos, J. Bertran, J. Am. Chem. Soc. 113 (1991) 2879. (f) Z. Lin, M.B. Hall, J. Am. Chem. Soc. 114 (1992) 6102. (g) S. Dapprich, G. Frenking, Angew. Chem. Int. Ed. Engl. 34 (1995) 354. (h) J. Li, R.M. Dickson, T. Ziegler, J. Am. Chem. Soc. 117 (1995) 11482. (i) J. Tomas, A. Lledos, Y. Jean, Organometallics 17 (1998) 190. (j) J. Tomas, A. Lledos, Y. Jean, Organometallics 17 (1998) 4932.

[9] (a) J.K. Burdett, M.R. Pourian, Organometallics 6 (1987) 1684. (b) J.K. Burdett, J.R. Phillips, M.R. Pourian, M. Poliakoff, J.J. Turner, R. Upmacis, Inorg. Chem. 26 (1987) 3054.

[10] R. Bau, M.H. Drabnis, Inorg. Chim. Acta 259 (1997) 27.

[11] M. Heinekey, W.J. Oldham Jr., Chem. Rev. 93 (1993) 913.

[12] (a) X.L. Luo, J.A.K. Howard, R.H. Crabtree, Magn. Reson. Chem. 29 (1991) S89. (b) D.G. Hamilton, R.H. Crabtree, J. Am. Chem. Soc. 110 (1988) 4126.

[13] T. Arliguie, B. Chaudret, R.H. Morris, A. Sella, Inorg. Chem. 27 (1988) 598.

[14] U. Bodensieck, A. Meister, G. Meister, G. Rheinwald, H. Stoeckli-Evans, G. Süss-Fink, Chimia 47 (1993) 189.

[15] G. Meister, G. Rheinwald, H. Stoeckli-Evans, G. Süss-Fink, J. Chem. Soc. Dalton Trans. (1994) 3215.

[16] L. Plasseraud, G. Süss-Fink, J. Organomet. Chem. 539 (1997) 163.

[17] T. Arthur, T.A. Stephenson, J. Organomet. Chem. 208 (1981) 369.

[18] G.M. Sheldrick, SHELXS-97, Program for Crystal Structure Determination, Acta Crystallogr. Sect A 46 (1990) 467.

[19] G.M. Sheldrick, SHELXL-97, Universität Göttingen, Göttingen, Germany, 1997.

[20] A.L. Spek, PLATON/PLUTON version Jan. 1999, Acta Crystallogr. Sect A 46 (1990) C34.

[21] Amsterdam Density Functional (ADF) program, release 2.3, Vrije Universiteit, Amsterdam, Netherlands, 1997.

[22] (a) E.J. Baerends, D.E. Ellis, P. Ros, Chem. Phys. 2 (1973) 41. (b) E.J. Baerends, P. Ros, Int. J. Quantum Chem. S12 (1978) 169. (c) P.M. Boerrigter, G. te Velde, E.J. Baerends, Int. J. Quantum Chem. 33 (1988) 87. (d) G. te Velde, E.J. Baerends, J. Comp. Phys. 99 (1992) 84.

[23] A.D. Becke, Phys. Rev. A 38 (1988) 3098.

[24] (a) J.P. Perdew, Phys. Rev. B 33 (1986) 8822. (b) J.P. Perdew, Phys. Rev. B 34 (1986) 7046.

[25] S.H. Vosko, L. Wilk, M. Nusair, Can. J. Phys. 58 (1980) 1200.

[26] L. Versluis, T. Ziegler, J. Chem. Phys. 88 (1988) 322.

[27] E.J. Baerends, Ph.D. Thesis, Vrije Universiteit, Amsterdam, Netherlands, 1975.